

Chromoelectric fields and quarkonium-hadron interactions at high energies

M. S. Kugeratski and F. S. Navarra

Instituto de Física, Universidade de São Paulo C.P. 66318, 05315-970 São Paulo, SP, Brazil

(Received 2 July 2004; revised manuscript received 20 April 2005; published 30 June 2005)

We develop a simple model to study the heavy quarkonium-hadron cross section in the high-energy limit. The hadron is represented by an external electric color field (capacitor) and the heavy quarkonium is represented by a small color dipole. Using high-energy approximations we compute the relevant cross sections, which are then compared with results obtained with other methods.

DOI: 10.1103/PhysRevC.71.065206

PACS number(s): 12.38.Lg, 12.40.Yx, 12.39.Mk

I. INTRODUCTION

Quarkonium-hadron cross sections ($\sigma_{\phi h}$) are a necessary tool to understand the forthcoming data on quarkonium production, which will become available at Brookhaven National Laboratory's Relativistic Heavy Ion Collider (RHIC). In the past six years many efforts have been devoted to this problem [1] and real progress has been achieved, especially for cross sections at low energies, close to the dissociation threshold. In the energy region far from threshold the situation is less clear and even the energy dependence is still a subject of debate. Extrapolations from calculations valid at low energies points in different directions. Results obtained with the nonrelativistic quark model [2] indicate a rapidly falling cross section. This behavior is due to the Gaussian tail of the quark wave functions used in the quark exchange model. This same behavior could be found within chiral meson Lagrangian approaches with the introduction of \sqrt{s} -dependent form factors [3]. In QCD sum rules [4] the cross section was found to be monotonically increasing with energy.

Calculations of $\sigma_{\phi h}$ designed to be valid at high energies ($\sqrt{s} \simeq 20$ GeV) are quite few: the Bhanot-Peskin (BP) approach [5–10], perturbative QCD plus geometrical extrapolation [11], the model of the stochastic vacuum (MSV) [12], and the light-cone dipole formalism [13]. During the past few years the leading-order BP approach has been used most often. However, the recent next-to-leading-order calculations presented in [10] show that, for charmonium, the formalism breaks down because this system is not heavy enough. Most of the calculations mentioned here predict a rising cross section. In Ref. [9], $\sigma_{\phi h}$ falls with energy and in Ref. [12] it stays constant.

If the quarkonium is treated as an ordinary hadron, its cross section for interaction with any other ordinary hadron must increase smoothly at higher energies, in much the same way as the proton-proton or pion-proton cross sections. The underlying reason is the increasing role played by perturbative QCD dynamics and the manifestation of the partonic nature of all hadrons. However, this partonic picture starts to be dominant only at much higher energies ($\sqrt{s} > 100$ GeV). In the energy region relevant for RHIC physics nonperturbative aspects are still very important. In the aforementioned high-energy calculations, different nonperturbative ingredients were employed: moments of the gluon distribution in the hadron

[5–10], hadron and quarkonium wave functions [11], and QCD vacuum expectation values (condensates) [12].

Since there are still discrepancies concerning numbers (which may vary by one order of magnitude for different estimates) and the energy behavior, we think that it is interesting to calculate $\sigma_{\phi h}$ with a nonperturbative approach, putting emphasis on the role played by the chromoelectric fields. In [14] a similar treatment was adopted to study the quarkonium dissociation inside a QCD plasma. The color electric fields appearing in the transition matrix element were related to the color charge density of the medium, which, in turn, was computed in a specific model of the QGP. Here we start with a similar expression for the transition amplitude but, because we are in a purely hadronic phase, we must know the chromoelectric field inside nucleons and pions. There has been progress in the study of these fields, coming from models of the QCD vacuum [15], lattice QCD [16], the field correlator method (FCM) [17], and Coulomb gauge QCD [18]. We hope that we can benefit from these advances and use the profiles of the chromoelectric fields estimated in these works in our problem. For this purpose, we treat the interaction between the quarkonium and hadron as being analogous to the interaction of a small dipole traversing a large capacitor and interacting with the color electric field but not with its sources. In the final part of this work we discuss the validity of this last assumption. Using a contact interaction between a heavy quark (or antiquark) and a quark (or antiquark) we compute the corresponding cross section and find that it is indeed much smaller than the heavy quark-external field cross section. The model developed here bears some resemblance to the BP picture but is much simpler. Some simplifying assumptions are used to render the calculations quasi-analytic and preserve the understanding of the basic physics.

II. THE MODEL**A. The interaction Hamiltonian**

The starting point is the assumption that the quarkonium (dipole) is small compared with the hadron (capacitor). As a consequence, the \bar{Q} - Q pair will interact mostly with the external color field but not with the (quark) sources. Moreover, the external color field is considered to have only

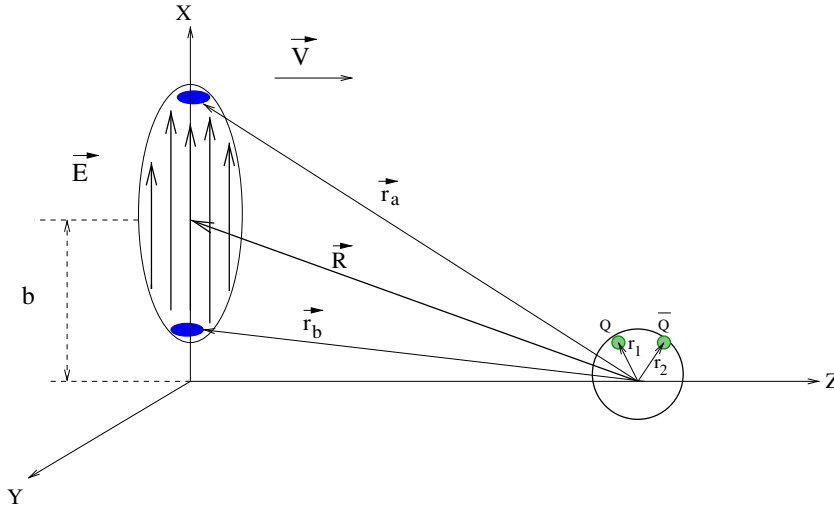


FIG. 1. (Color online) Quarkonium-hadron interaction in the quarkonium rest frame. The hadron is a capacitor moving to the right. The \vec{E}^a field is along the x direction. The thick black dots are the capacitor “plates:” quark-antiquark for the pion and quark-diquark for the proton.

low momentum components (“soft gluons”) and thus is able to transfer only a small amount of energy, which will be barely enough to dissociate the bound state. In the case of the charmonium, the typical binding energy is $\epsilon \simeq 0.6$ GeV. Therefore, in a first approximation

$$\epsilon \ll M_\Phi, \quad (1)$$

where M_Φ is the mass of the bound state ($M_\Phi \simeq 3$ GeV). In the case of the bottomonium this approximation is even better. The binding energy is also small compared to the collision energy,

$$\epsilon \ll \sqrt{s}. \quad (2)$$

Inequality (1) justifies the use of quantum mechanical perturbation theory (the Born approximation) and inequality (2) justifies the use of the eikonal approximation, which, in this case, implies that the hadron follows a straight-line trajectory and remains essentially undisturbed during the interaction. In Fig. 1 we present our picture of the scattering and our choice of coordinates, in the quarkonium rest frame: \vec{r}_1 and \vec{r}_2 are the quark and antiquark coordinates and \vec{E}^a is the chromoelectric field in the projectile, which will be a proton or a pion, moving with constant velocity \vec{v} at impact parameter \vec{b} .

With these assumptions we can write the interaction Hamiltonian as

$$H_{\text{int}} = g(T_1^a \vec{E}_1^a \vec{r}_1 + \bar{T}_2^b \vec{E}_2^b \vec{r}_2), \quad (3)$$

where T^a (\bar{T}^b) are the generators of color group SU(3) in the fundamental (conjugate) representation; \vec{E}_1^a and \vec{E}_2^b are the chromoelectric fields generated by the hadron in motion (capacitor) and “felt” by quark and antiquark in the bound state, respectively. They have to be Lorentz transformed to the quarkonium rest frame, bringing to our calculation a Lorentz gamma factor, which is the source of the energy dependence (\sqrt{s}) of our results. We shall for the moment neglect the magnetic component, since it does not do any work on the charges and thus is not effective in the energy transfer. Besides, the magnetic interaction is inversely proportional to the quark mass, and so is suppressed.

We can represent this external field by

$$\vec{E}^a(r_e, t) = \gamma \vec{E}_0^a \exp \left[-\frac{(X - x_e)^2}{d^2} - \frac{(Y - y_e)^2}{d^2} \right] \times \exp \left[-\gamma^2 \frac{(vt - z_e)^2}{d^2} \right], \quad (4)$$

with $e = 1, 2$. X , Y , and Z are the hadron coordinates and γ is the usual Lorentz factor. $Z = vt$, because the hadron moves with velocity \vec{v} along the z axis. \vec{E}_0^a , which will be abbreviated by E , is the color electric field at the center of the projectile. The projectile mean-square radius is related to the parameter d through

$$\sqrt{\langle r_h^2 \rangle} = 0.86 d.$$

We neglect the deflection of the hadron trajectory, because we are studying reactions in the high-energy and nonperturbative regime (i.e., with low momentum transfer). X and Y are related to the impact parameter b by $b^2 = X^2 + Y^2$. Notice that, for simplicity, we choose one preferential direction for the field, in this case, the x axis.

Neglecting the c.m. motion, we can rewrite (3) as

$$H_{\text{int}} = g \left(\frac{\lambda^a}{2} E_1^a + \frac{\lambda^{b^T}}{2} E_2^b \right) \left(\frac{x_1 - x_2}{2} \right). \quad (5)$$

Also for the sake of simplicity, when working with (5), we will take $x_1 - x_2 \simeq a$, where a is the typical separation between quark and antiquark. Initially, the quark-antiquark pair is in a localized region of space.

B. The initial state

The initial wave function of the system has spatial and color parts defined by

$$\Psi_i = f(r_1, r_2) c_n d_n, \quad (6)$$

where c_n and d_n , with $n = 1, 2, 3$, are the initial color vectors [19] for quark and antiquark, respectively, taken in a color

singlet state. We choose

$$f(r_1, r_2) = N_i \exp\left[-\frac{\vec{r}_1^2}{a^2}\right] \exp\left[-\frac{\vec{r}_2^2}{a^2}\right] \exp(-i\varepsilon_i t), \quad (7)$$

where ε_i ($\varepsilon_i = M_\Phi$) is the quarkonium initial energy and N_i is a normalization constant given by

$$N_i^2 = \left(\frac{2}{\pi}\right)^3 \frac{1}{a^6}.$$

The initial wave function Ψ_i describes the confinement of quarks and also asymptotic freedom, as it allows the quarks to be independent inside the bag. It is easy to see that the connection between the quarkonium mean-square radius and the parameter a is

$$\sqrt{\langle r_{Q\bar{Q}}^2 \rangle} = 1.09 a.$$

C. The final state

Under the action of the external field the initial wave function Ψ_i evolves to a final state Ψ_f :

$$\Psi_f = t(r_1, r_2) c_j d_k, \quad (8)$$

where c_j and d_k , with $j, k = 1, 2, 3$, are the quark and antiquark final color vectors, respectively, and $t(r_1, r_2)$ is the spatial part of the wave function. In the final state of this reaction we have to deal with the transition of a pair of an excited quark and an antiquark to a pair of mesons $D\bar{D}$ (or $B\bar{B}$). This transition is highly nonperturbative and has to be modeled. We shall use two approaches.

1. Model A

We first assume that the quark and antiquark are converted into two free mesons (a M and a \bar{M}), which are thus described by plane waves

$$t_A(r_1, r_2) = N_A \exp(i\vec{p}_1 \cdot \vec{r}_1) \exp(i\vec{p}_2 \cdot \vec{r}_2) \exp(-i\varepsilon_f t), \quad (9)$$

where \vec{p}_1 and \vec{p}_2 are the meson momenta and N_A is a normalization constant given by

$$N_A^2 = \frac{1}{V^2},$$

with V being an arbitrary normalization volume, which will be canceled in the calculation of the cross section. In Eq. (9) ε_f is the final energy of the $Q\bar{Q}$ pair. The energy transferred during the reaction must be sufficient to dissociate the bound state into a pair of mesons with open charm ($D\bar{D}$) or beauty ($B\bar{B}$) and therefore

$$\varepsilon_f = \sqrt{(\vec{p}_1)^2 + m_M^2} + \sqrt{(\vec{p}_2)^2 + m_{\bar{M}}^2}, \quad (10)$$

where m_M ($m_{\bar{M}}$) is the mass of the meson resulting from the fragmentation of the quark (antiquark). With this definition of ε_f we implicitly account for the conversion of quarks into hadrons, a process that cannot be better described in this simple model.

The assumptions (9) and (10) are reasonable but they represent a case of “extreme freedom”: They do not take

into account the energy loss from a parent quark when it is converted to a (less energetic) final meson. This process is described, in certain situations, by the fragmentation functions. Moreover, the final mesons can have any momentum and even though higher momenta will be naturally suppressed in the calculation, we are overestimating the phase space of the reaction.

2. Model B

Given these weak points of (9) and (10) we shall also use a second, more conservative approach for the final state. We shall assume that the energy transferred to the heavy quarkonium Φ will transform it into an excited (but still bound) state Φ' . The mass of this excited state will be taken to be slightly higher than the first charmonium and bottomium excitations, Ψ' and Υ' , respectively. It is known that these excitations are very weakly bound. Therefore, by choosing slightly higher masses for them, which are above the $D\bar{D}$ and $B\bar{B}$ decay thresholds, we are simulating a fragmentation process to a pair of nearly at rest mesons. This assumption is complementary to (9) and (10) since here we give to the heavy quarks only the “minimal freedom.” The ground-state wave function was chosen to be the Gaussian (7). Taking the harmonic oscillator as inspiration, we choose the wave function of the first excited state as a function that is odd in the x direction (the direction of the chromoelectric field) and symmetric in x_1 and x_2 :

$$t_B(r_1, r_2) = N_B \frac{x_1 + x_2}{2} \exp\left[-\frac{\vec{r}_1^2}{a'^2}\right] \times \exp\left[-\frac{\vec{r}_2^2}{a'^2}\right] \exp(-i\varepsilon_f t), \quad (11)$$

where the normalization constant is

$$N_B^2 = \left(\frac{4}{\pi}\right)^3 \frac{1}{a'^8}$$

and a' is related to the size of the state Ψ' or Υ' . Using the wave function (11) has some advantages. First, it avoids the definition of a fragmentation mechanism with the introduction of new parameters. Second, as can be seen, (11) is orthogonal to (9), so that the matrix element $\langle \Psi_f | H_{\text{int}} | \Psi_i \rangle$ is zero if the Hamiltonian is a constant. Notice that this does not happen when we use (9) and therefore approach A might contain spurious contributions. The same comment is valid for the calculations made in Ref. [14]. This makes the contrast between approaches A and B even more necessary. Finally, in what follows we shall use the Hamiltonian (3), without the approximation $x_1 - x_2 \simeq a$ made in model A.

3. Transition amplitudes and cross sections

The transition amplitude for model A can be easily computed from (5), (4), (6), (8), and (9):

$$\begin{aligned} T_{fi} &= \langle \Psi_f | H_{\text{int}} | \Psi_i \rangle \\ &= \int dt \int d^3\vec{r}_1 \int d^3\vec{r}_2 \Psi_f^*(\vec{r}_1, \vec{r}_2) \\ &\quad \times H_{\text{int}}(\vec{r}_1, \vec{r}_2) \Psi_i(\vec{r}_1, \vec{r}_2). \end{aligned} \quad (12)$$

An analogous expression holds for model B with the use of (3), (4), (6), (8), and (11). We next take the amplitude squared, $|T_{fi}|^2 = T_{fi}^* T_{fi}$, and since color is not observed, we take the average of the all initial color states and the sum of all final states:

$$|T_{fi}|^2 \rightarrow \overline{|T_{fi}|^2} \equiv \frac{1}{3} \sum_n \frac{1}{8} \sum_a \sum_j \sum_k |T_{fi}|^2. \quad (13)$$

The cross section with model A is given by

$$\sigma_A = \int \frac{V}{(2\pi^3)} d^3 p_1 \int \frac{V}{(2\pi^3)} d^3 p_2 2\pi \int_0^\infty db b \overline{|T_{fi}|^2}. \quad (14)$$

This expression is very simple and can almost be calculated analytically. Because of the Gaussian ansatz (4) and (6) we can easily integrate (12) over the coordinates and over the impact parameter. In the last step of (14), the integration over the phase space had to be done numerically. In [20] we made the additional assumption that the outgoing mesons are nearly at rest and we could thus simplify (10) and perform the integration over \vec{p}_1 and \vec{p}_2 analytically. Here we prefer to be more “exact” and perform the last integrations numerically.

The cross section with model B is simply given by

$$\sigma_B = 2\pi \int_0^\infty db b \overline{|T_{fi}|^2}, \quad (15)$$

which, after the proper substitutions and integrations yields

$$\begin{aligned} \sigma_B &= \frac{32}{3} \pi^5 \langle g E_0 \rangle^2 \frac{\gamma^2}{\gamma^2 - 1} \\ &\times \frac{d^{10} a'^8 a^{10}}{(a^2 + a'^2)^5 [a'^2 a^2 + d^2 (a^2 + a'^2)]^3} \\ &\times \exp\left(-\omega^2 \frac{\gamma^2 a^2 a'^2}{2(\gamma^2 - 1)} + d^2\right), \end{aligned} \quad (16)$$

where

$$\omega = \varepsilon_f - \varepsilon_i = M_\Phi - M_\phi. \quad (17)$$

From Eq. (16) we can observe that the cross section rises with the energy (γ) and saturates at a constant value. The enhancement of the chromoelectric field is tamed by the Lorentz contraction of the projectile. As for the size parameters, a , a' , and d , the cross section first rises and then falls with increasing values of the parameters. The values of the maxima strongly depend on the model and might change for a different choice of wave functions. However, the physical picture is very simple. Expression (16) tells us that the probability of converting a quarkonium of given initial size a to a final state with size a' tends to zero if $a' = 0$ or if $a' \rightarrow \infty$ because the overlap between these very different states and the initial state is zero. For the same reason the cross section vanishes for $a = 0$ and for $a \rightarrow \infty$. The parameter d is associated with the extension of the capacitor. In the limit when $d \rightarrow \infty$ the spatial dependence of the potential

disappears and it becomes a constant and then $\langle \Psi_f | H_{\text{int}} | \Psi_i \rangle \rightarrow \langle \Psi_f | \Psi_i \rangle = 0$.

D. Interaction with the sources

In the introduction it was assumed that the quarkonium is well represented by a small dipole, which traverses a large capacitor. However, this may be too strong of an assumption because the dipole is not always so small. For example, comparing the size of the charmonium with the size of pion we have typically $a/d \simeq 0.4/0.6 \simeq 0.67$. Therefore it is necessary to include the interaction between the quark and antiquark in the quarkonium with the sources (the “plates” of the capacitor), which may be either a quark and an antiquark in the case of the pion or a quark and a diquark in the case of the proton.

To take these interactions into account we shall assume that the interaction between a quark (or diquark) in the capacitor and a charm quark (or antiquark) in the dipole can be divided into a short-distance part and a long-distance part. The latter was already included before in the interaction with the chromoelectric fields produced by the sources. The former will be modeled as follows.

1. Model C

The short-distance interaction can be approximated by the contact interaction part (the one with the delta function) of the one-gluon exchange potential [21]:

$$\begin{aligned} H_{\text{int}} = V_{\text{OGE}} &= \sum_{i=a,b} \sum_{j=1,2} \frac{\alpha_s}{4} \vec{\lambda}_i \cdot \vec{\lambda}_j \\ &\times \left[\frac{1}{r_{ij}} - \frac{2\pi}{3m_i m_j} \vec{\sigma}_i \cdot \vec{\sigma}_j \delta^3(\vec{r}_{ij}) \right], \end{aligned} \quad (18)$$

where λ and σ are the Gell-Mann and Pauli matrices, respectively, which are responsible for color and spin interactions. The Coulomb term in this expression will be neglected because it is of long range. The labels $i = a, b$ and $j = 1, 2$ refer to particles in the capacitor and dipole, respectively. With this notation, in the interaction between particle a and 1 the delta function takes the form

$$\delta^3(\vec{r}_a - \vec{r}_1) = \delta(x_a - x_1) \times \delta(y_a - y_1) \times \delta(z_a - z_1), \quad (19)$$

where $\vec{r}_1 = (x_1, y_1, z_1)$ is the same as before and $\vec{r}_a = (x_a, y_a, z_a)$ is the coordinate of particle a in the quarkonium rest frame. To compute the transition amplitude we need to know the new wave functions, which now include both the quarkonium and the capacitor. They are

$$\Psi_i = f(\vec{r}_1, \vec{r}_2) g(\vec{r}_a, \vec{r}_b) c_n d_n e_m h_m \quad (20)$$

and

$$\Psi_f = t_C(\vec{r}_1, \vec{r}_2) g(\vec{r}_a, \vec{r}_b) c_i d_j e_l h_k. \quad (21)$$

In Eq. (20) the function f is the same as before and is given by (7). The function t_C in Eq. (21) represents the spatial distribution of the heavy quarks in the final state, which is assumed to be an excited but still bound state, very much

like in model B. However, if we would choose $t_C = t_B$, the transition amplitude $\langle \Psi_f | H_{\text{int}} | \Psi_i \rangle$ would vanish because the contact interaction does not depend on the coordinates and hence $\langle \Psi_f | \Psi_i \rangle$ is the product of an odd and an even function of x and is thus zero. Since we are mostly interested in knowing the order of magnitude of this contact interaction we shall approximate the final-state wave function by a Gaussian, given by

$$t_C(\vec{r}_1, \vec{r}_2) = N_C \exp\left(\frac{-r_1^2}{a^2}\right) \exp\left(\frac{-r_2^2}{a'^2}\right) e^{-i\varepsilon_f t}, \quad (22)$$

with the normalization constant given by

$$N_C^2 = \left(\frac{2}{\pi}\right)^3 \frac{1}{a^6}. \quad (23)$$

The computation of the contact interaction requires knowledge of the positions of the quarks in the capacitor, which is given by the function

$$\begin{aligned} g(\vec{r}_b, \vec{r}_b) = N_P \exp\left[\frac{-(x_a - X)^2}{d^2}\right] \exp\left[\frac{-(y_a - Y)^2}{d^2}\right] \\ \times \exp\left[\frac{-(x_b - X)^2}{d^2}\right] \exp\left[\frac{-(y_b - Y)^2}{d^2}\right] \\ \times \exp\left[\frac{-\gamma^2(z_a - Z)^2}{d^2}\right] \exp\left[\frac{-\gamma^2(z_b - Z)^2}{d^2}\right], \end{aligned} \quad (24)$$

where $Z = vt$, d and γ have the same meaning as before, and N_P is the normalization constant of the projectile wave function, given by

$$N_P^2 = \frac{8\gamma^2}{\pi^3 d^6}. \quad (25)$$

Notice that g is the same in the initial and in the final state. This assumption is consistent with the eikonal approximation previously introduced and avoids the introduction of new parameters.

With these ingredients we can evaluate the transition amplitude,

$$\begin{aligned} T_{fi} = \langle \Psi_f | H_{\text{int}} | \Psi_i \rangle = \int dt \int d^3\vec{r}_1 d^3\vec{r}_2 \int d^3\vec{r}_a d^3\vec{r}_b \Psi_f^* \\ \times (\vec{r}_1, \vec{r}_2, \vec{r}_a, \vec{r}_b) H_{\text{int}}(\vec{r}_1, \vec{r}_2, \vec{r}_a, \vec{r}_b) \\ \times \Psi_i(\vec{r}_1, \vec{r}_2, \vec{r}_a, \vec{r}_b), \end{aligned} \quad (26)$$

and the cross section,

$$\begin{aligned} \sigma_C = \frac{2^{10}}{3^4} \pi \alpha_s^2 \left(\frac{1}{m_a m_1} + \frac{1}{m_a m_2} + \frac{1}{m_b m_1} + \frac{1}{m_b m_2} \right)^2 \\ \times \frac{\gamma^2}{\gamma^2 - 1} \frac{a^6 a'^6}{(a'^2 + a^2)^5 [d^2(a'^2 + a^2) + 2a^2 a'^2]} \\ \times \exp\left(-\omega^2 \frac{\gamma^2 a^2 a'^2}{(a'^2 + a^2) + d^2}\right), \end{aligned} \quad (27)$$

where we have used (13) and the analogous expression for the sum and average over spins. Apart from a numerical factor, (16) and (27) have the same energy dependence. This is so

because the same Lorentz contraction in the exponent of the Hamiltonian (3) and (4) leading to (16) is now present in the capacitor wave function (24). Moreover, the same Lorentz γ factor, previously multiplying the \vec{E}^a field in (4), reappears now in the normalization constant (25). The dependence of (27) on a and a' is qualitatively the same as the one found in (16) and has the same physical origin. Finally, the cross section in Eq. (27) is now a monotonically decreasing function of d . The observed behavior with d means that, in a larger capacitor, the quarks are spread across a larger transverse area and it becomes more difficult for them to find the charm quarks in the target and suffer a contact interaction.

III. RESULTS AND DISCUSSION

In the numerical estimates presented in the following, we shall adopt $d = 0.8$ and 0.6 fm for the proton and the pion, respectively. We shall also take $a = 0.4$ and 0.2 fm for the J/ψ and Υ' , respectively, and $a' = 0.8$ and 0.45 fm for the Ψ' and Υ' , respectively. The bound states Ψ ($m_\Psi = 3.07$ GeV) and Υ' ($m_{\Upsilon'} = 9.46$ GeV) will be, in model A, dissociated into pairs of mesons D ($m_D = 1.87$ GeV) and B ($m_B = 5.27$ GeV). The excited states used in models B and C have masses $m_\Phi = 3.8$ GeV and $m_\Phi = 11$ GeV in the case of charmonium and bottomonium, respectively. The value of the strong coupling constant and the constituent quark masses are the same as used in [21] (i.e., $\alpha_s = 0.64$, $m_q = 0.3$ GeV, $m_c = 1.2$ GeV, and $m_b = 4.74$ GeV) and the diquark mass is $m_d = 0.60$ GeV.

As is clear from (5) and (4), we need to know the average value of the color electric field in the projectile $gE = \langle h | gE | h \rangle$. In a first approximation this number might be identified with the string tension $\kappa \simeq 0.18$ GeV² or $\kappa \simeq 0.9$ GeV/fm. The string tension calculated in [18] is somewhat larger. In [17] the transverse profile of the string was studied. The strength of $\langle h | gE | h \rangle$ depends on the quark-antiquark (or quark-diquark) separation, it is larger for larger systems and so far it has been calculated only for large systems. Therefore $\langle h | gE | h \rangle$ is another source of differences between a proton and a pion projectile. Taking an average of the values found in [17] we choose $\langle h | gE | h \rangle = 1$ GeV/fm.

As mentioned in the introduction, our model has common aspects with the BP approach. Therefore we shall, in what follows, compare our results for $\sigma_{\Phi h}$ with those obtained by Kharzeev in [7]:

$$\sigma_{\Phi h} = 2.5 \left(1 - \frac{\lambda_0}{\lambda}\right)^{6.5} \text{ mb} \quad (28)$$

with λ given by

$$\lambda \simeq \frac{(s - M_\Phi^2)}{2M_\Phi} \quad (29)$$

and $\lambda_0 \simeq (M_h + \varepsilon)$, where M_h is the projectile mass and

$$\varepsilon = 2m_M - M_\Phi. \quad (30)$$

In Fig. 2 we show the cross sections for the proton-charmonium dissociation obtained with model A (dotted lines) and model B (dashed lines) and compare them with the BP

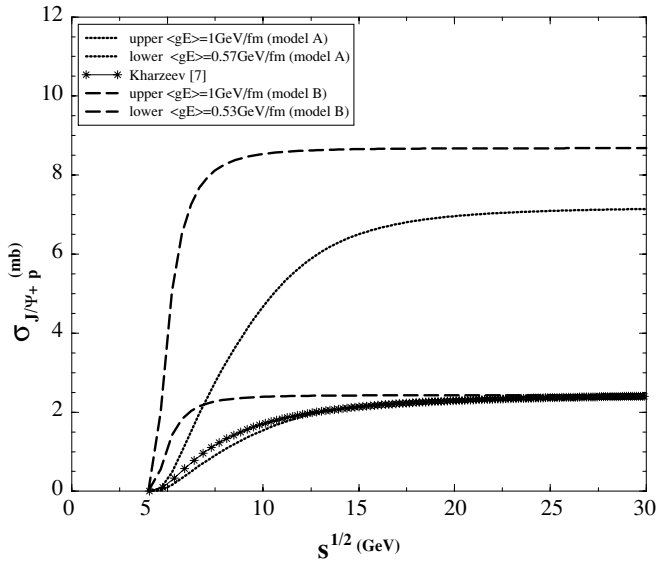


FIG. 2. $J/\psi + p$ cross section with model A (dotted lines), with model B (dashed lines), and with the Bhanot-Peskin approach (lines with stars). Upper curves: stronger \vec{E}^a field. Lower curves: weaker \vec{E}^a field.

cross section (solid line with stars) given by (28). The two upper curves are obtained with $\langle h|gE|h \rangle = 1$ GeV/fm and the two lower curves with $\langle h|gE|h \rangle = 0.57$ GeV/fm (model A) and $\langle h|gE|h \rangle = 0.53$ GeV/fm (model B). With these smaller values of the chromoelectric field our curves come close to (28). Figure 3 shows the corresponding cross sections for the proton-bottomonium dissociation. Again, the two upper curves are obtained with $\langle h|gE|h \rangle = 1$ GeV/fm and the two lower curves with $\langle h|gE|h \rangle = 0.69$ GeV/fm (model A) and $\langle h|gE|h \rangle = 0.49$ GeV/fm (model B). As in the previous figure, reducing the value of $\langle h|gE|h \rangle$ leads to some agreement with (28). Given the conceptual resemblance between our model

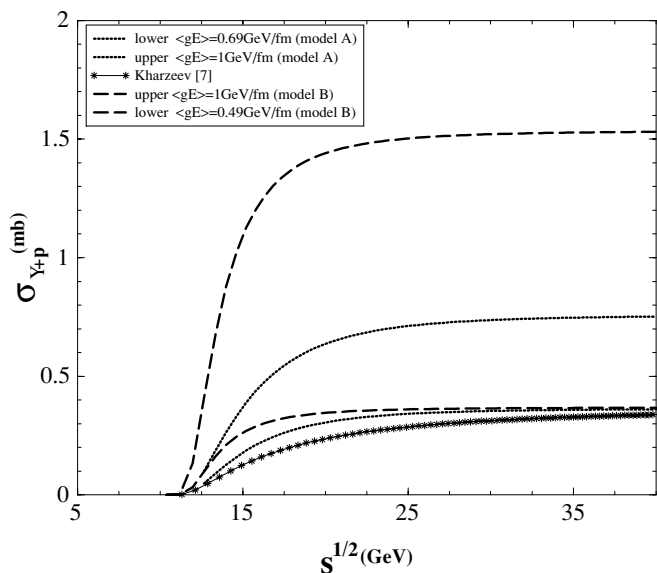


FIG. 3. Same as Fig. 2 for the $\Upsilon + p$ cross section.

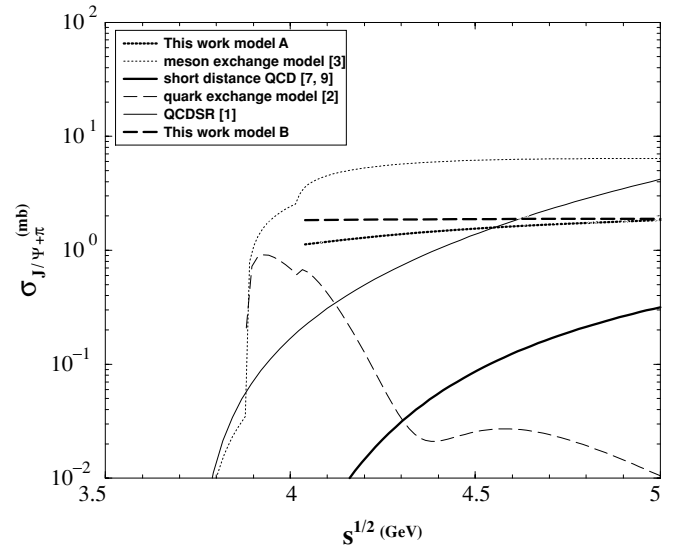


FIG. 4. Pion-charmonium cross section as a function of \sqrt{s} with several models.

and the BP one, it is reassuring to find a certain similarity between the results, both in magnitude and energy behavior, once an appropriate value of $\langle h|gE|h \rangle$ is chosen.

In Fig. 4 we show the cross section for J/ψ dissociation by pions compared with results obtained with the meson exchange model [3] (thin dotted line), the quark exchange model [2] (thin long dashed line), short-distance QCD [the BP approach; Eq. (28)] (thick solid line), and QCD sum rules [1] (thin solid line). In spite of the fact that at such low energies our approach loses validity, it is, nevertheless, interesting to observe that our curve is in the center of the region covered by the other calculations. In Fig. 5 we compare the cross sections $p + J/\psi$

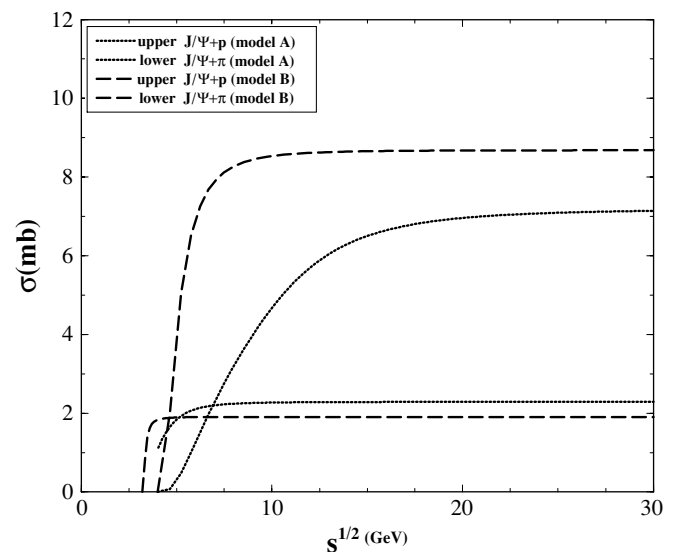


FIG. 5. Charmonium-hadron cross section with model A (dotted lines) and model B (dashed lines). Upper curves: $\sigma_{J/\psi} + p$. Lower curves $\sigma_{J/\psi} + \pi$.

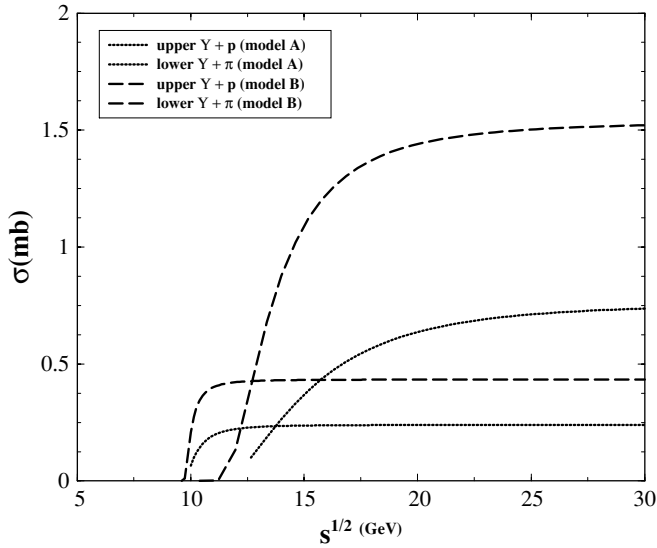


FIG. 6. Same as Fig. 5 for bottomonium-hadron cross sections.

(upper curves) and $\pi + J/\psi$ (lower curves) calculated with models A (dotted lines) and B (dashed lines). In the high-energy limit, where both cross sections are nearly constant, we observe that the relation between the cross sections is

$$\sigma_{p-\Phi} \simeq 3\sigma_{\pi-\Phi} \quad (\text{model A}), \quad (31)$$

$$\sigma_{p-\Phi} \simeq 4.2\sigma_{\pi-\Phi} \quad (\text{model B}), \quad (32)$$

which in both cases is much larger than the one expected from the additive quark model:

$$\sigma_{p-\Phi} \simeq \frac{3}{2}\sigma_{\pi-\Phi}. \quad (33)$$

This is remarkable since the additive quark model relation holds for other high-energy scattering processes such as $\pi-p$ and $p-p$. Since $\langle h|gE|h\rangle$ was kept the same for both cases, this unexpected relation between the cross sections must come from differences in the wave functions. In Fig. 6 we repeat this comparison for the reactions $p + \Upsilon$ and $\pi + \Upsilon$, finding (31) for both models. We have kept $\langle h|gE|h\rangle = 1 \text{ GeV/fm}$ for both projectiles. Taking $\langle p|gE|p\rangle > \langle \pi|gE|\pi\rangle$ would increase the deviation from (33).

In the high-energy limit ordinary hadrons are expected to have a geometrical total cross section. Since the quarkonium dissociation discussed here is a more specific reaction it is not obvious that its cross section follows a geometrical behavior. Such a behavior was found in [8]: $\sigma_{\Phi h} \propto \alpha_s a_0^2$, where a_0 is the Bohr radius of the quarkonium. In our case, as can be seen from (16), (27), and the numerical evaluation of (14), we have a very nontrivial dependence on a . Since the initial state (containing the variable a) is the same, the difference between models comes from the spatial dependence of the final state. The plane waves in model A have no spatial scale. Therefore they are more “inclusive” and so σ_A should be closer to the quarkonium-hadron total cross section than σ_B . In model B the quarkonium ground state is converted into a resonancelike state, the wave function of which contains the size parameter

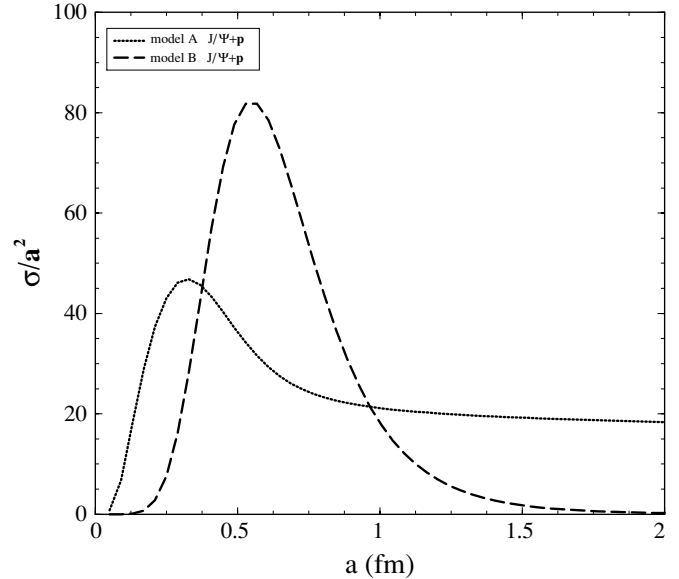


FIG. 7. Charmonium-hadron cross sections as a function of the charmonium size parameter for model A (dotted line) and for model B (dashed line).

of the resonance and distorts the final geometrical behavior. Therefore model A is closer to a geometrical behavior than model B.

To see how far we are from the geometrical behavior, we show in Figs. 7 and 8 the dependence of σ_A (dotted line) and σ_B (dashed line) on a for charmonium (Fig. 7) and bottomonium (Fig. 8) dissociation. The cross sections are divided by a^2 so that geometrical behavior translates into a horizontal line. We see that, whereas model A tends to this behavior, model B is far from a geometrical behavior. This indicates again that our model is very sensitive to the choice of the final-state wave functions.

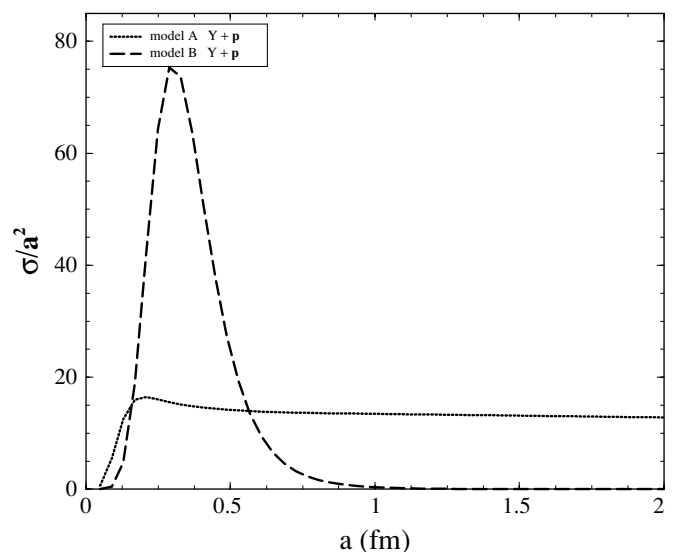


FIG. 8. Same as Fig. 7 for bottomonium-hadron cross sections.

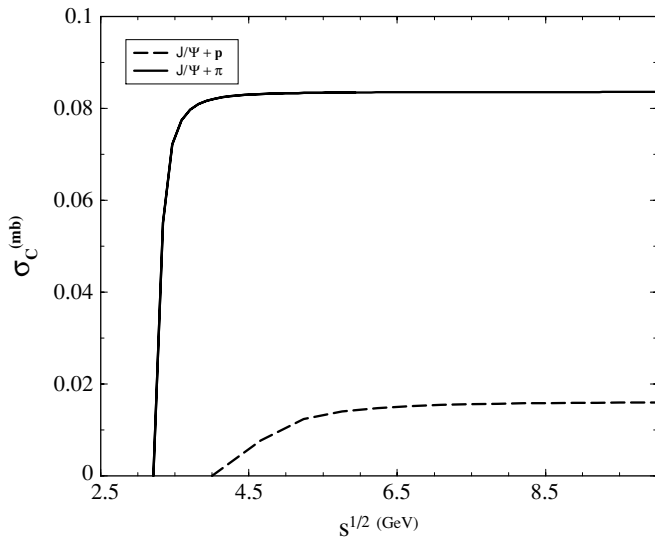


FIG. 9. Charmonium-proton (dashed line) and charmonium-pion (solid line) cross sections calculated with model C (contact interactions).

In Fig. 9 we show the cross section σ_C (27) for charmonium dissociation by protons (solid line) and by pions (dashed line). In Fig. 10 we show the same quantity for bottomonium dissociation. We use the central values for a , a' , d , and α_s . We can see that, in all processes, the cross sections are more than two orders of magnitude smaller than the corresponding cross sections computed with model A or model B. No possible change in parameters could make these cross sections comparable. Another feature of these curves is that the cross sections for J/ψ dissociation by pions are larger than those for protons by a factor close to 4. This might be guessed by looking at (27). The pion is a light quark-antiquark system and the proton is a light quark-diquark dipole. The diquark is twice as heavy as a constituent quark. Whereas for the pion $m_b = m_a$, for the proton we have $m_b = 2m_a$.

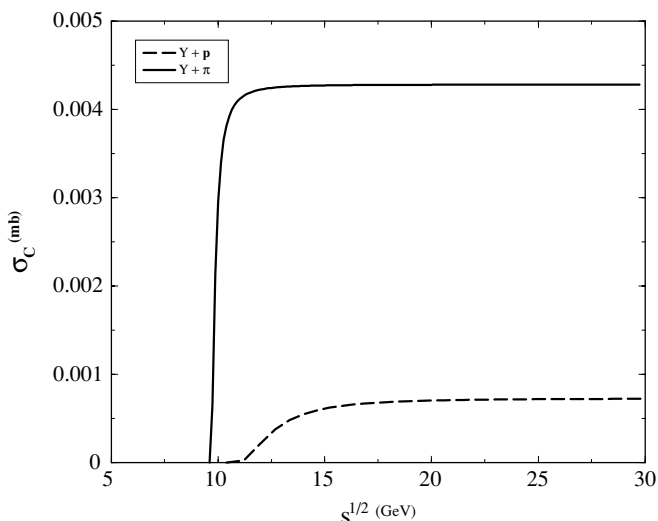


FIG. 10. Same as Fig. 9 for bottomonium-hadron cross sections.

Before concluding we need remark on medium effects on the cross sections calculated here. We are primarily studying reactions that happen before thermalization (in nucleus-nucleus collisions) or with no thermalization at all (in proton-nucleus collisions). The formation time of the heavy quark pair is of the order of 0.2 fm. The thermalization time of hadronic matter formed in heavy-ion collisions is a model-dependent quantity. Early estimates pointed to 1 fm. Recent estimates [23] point to 0.6 fm. Even if we take seriously this last number, it is fair to say that heavy quark pair production (and collision with a hadron at high energies) precedes the formation of an equilibrated medium. After thermalization, the energy is completely redistributed and collisions occur at energies of the order of the temperature (<1 GeV). In this regime we do not expect our approach to be valid. The effects of a thermal medium on heavy quarkonium are known [24]: The string tension becomes weaker, the quarkonium size increases, and its mass decreases. These effects are all very small except close to the deconfinement transition temperature. In view of these considerations we have neglected medium effects in our calculations.

IV. CONCLUSIONS

We have developed a simple model for the nonperturbative quarkonium-hadron interaction. At the present stage of the field, this sort of model remains useful for organizing our ideas. We tried to make simple and yet realistic choices for the interaction Hamiltonian and for the wave functions. In particular, we have treated the final state in two very different and complementary ways. Simple models are in appropriate for providing very precise results but they can help in determining the order of magnitude of the cross sections and their behavior with the reaction energy. Having said that, we can summarize our conclusions as follows:

- (i) The charmonium-hadron cross section is about a few millibarns. The bottomonium-hadron cross section is about one-quarter as large. This is in agreement with most of the previous calculations.
- (ii) All cross sections grow with the reaction energy and reach a plateau in the high-energy limit. This is in agreement with the BP approach.
- (iii) In this limit they do not obey the simple relations derived from the additive quark model.
- (iv) Also in this limit our cross sections deviate significantly from the geometrical behavior ($\sigma \propto a^2$).
- (v) The contact interactions between the heavy quarks and the light quarks in the light hadrons is negligible compared to the long-distance quark- \vec{E}^a field interaction. This is surprising since sometimes the dipole and the capacitor have similar sizes. This finding gives a posteriori support to our model and also to the BP approach.

Conclusion (i) may be relevant for RHIC and Large Hadron Collider (LHC) physics. Conclusions (ii), (iii), and (iv) suggest that heavy quarkonium has interaction properties

that are very different from light hadrons. This has been conjectured before. In particular, in [22] this difference was attributed to the fact that in heavy quarkonium the energy is mainly stored in the masses whereas in light hadrons the energy (mass of the hadron) comes mostly from the gluonic fields.

ACKNOWLEDGMENTS

We are indebted to M. Nielsen, D.A. Fogaça, and F. Durães for fruitful discussions. This work has been supported by CNPq and FAPESP.

-
- [1] F. O. Duraes, H. Kim, S. H. Lee, F. S. Navarra, and M. Nielsen, *Phys. Rev. C* **68**, 035208 (2003).
- [2] C.-Y. Wong, E. S. Swanson, and T. Barnes, *Phys. Rev. C* **62**, 045201 (2000); **65**, 014903 (2001).
- [3] Y. Oh, T. Song, and S. H. Lee, *Phys. Rev. C* **63**, 034901 (2001).
- [4] F. S. Navarra *et al.*, *Phys. Lett.* **B529**, 87 (2002); M. Nielsen *et al.*, *Braz. J. Phys.* **33**, 316 (2003); F. O. Durães *et al.*, *Phys. Lett.* **B564**, 97 (2003).
- [5] M. E. Peskin, *Nucl. Phys.* **B156**, 365 (1979); G. Bhanot and M. E. Peskin, *Nucl. Phys.* **B156**, 391 (1979).
- [6] D. Kharzeev and H. Satz, *Phys. Lett.* **B366**, 316(1996); **B356**, 365 (1995); **B334**, 155 (1994).
- [7] D. Kharzeev, The Proceedings of the Enrico Fermi International School of Physics on “Selected Topics in Non-Perturbative QCD,” Varenna, Italy, June 1995, nucl-th/9601029.
- [8] F. Arleo, P.-B. Gossiaux, T. Gousset, and J. Aichelin, *Phys. Rev. D* **65**, 014005 (2001).
- [9] Y. Oh, S. Kim, and S. H. Lee, *Phys. Rev. C* **65**, 067901 (2002).
- [10] T. Song and S. H. Lee, hep-ph/0501252.
- [11] L. Gerland, L. Frankfurt, M. Strikman, H. Stoecker, and W. Greiner, *Phys. Rev. Lett.* **81**, 762 (1998).
- [12] H. G. Dosch, F. S. Navarra, M. Nielsen, and M. Rueter, *Phys. Lett.* **B466**, 363 (1999).
- [13] J. Hüfner, Y. P. Ivanov, B. Z. Kopeliovich, and A. V. Tarasov, *Phys. Rev. D* **62**, 094022 (2000).
- [14] B. Müller, nucl-th/9806023; S. C. Benzahra, *Phys. Rev. C* **61**, 064906 (2000).
- [15] M. Rueter and H. G. Dosch, *Z. Phys. C* **66**, 245 (1995).
- [16] T. T. Takahashi, H. Matsufuru, Y. Nemoto, and H. Suganuma, *Phys. Rev. Lett.* **86**, 18 (2001); T. T. Takahashi, H. Suganuma, Y. Nemoto, and H. Matsufuru, *Phys. Rev. D* **65**, 114509 (2002); T. T. Takahashi and H. Suganuma, *Phys. Rev. Lett.* **90**, 182001 (2003).
- [17] D. S. Kuzmenko and Y. A. Simonov, *Phys. Lett.* **B494**, 81 (2000); D. S. Kuzmenko, hep-ph/0204250.
- [18] P. O. Bowman and A. P. Szczepaniak, *Phys. Rev. D* **70**, 016002 (2004).
- [19] D. Griffiths, *Introduction to Elementary Particles* (John Wiley and Sons, New York, 1987), Chapter 9.
- [20] D. A. Fogaça, M. S. Kugeratski, and F. S. Navarra, *Braz. J. Phys.* **34**, 276 (2004).
- [21] J. Vijande, F. Fernandez, A. Valcarce, and B. Silvestre-Brac, *Eur. Phys. J. A* **19**, 383 (2004); S. Godfrey and N. Isgur, *Phys. Rev. D* **32**, 189 (1985).
- [22] F. O. Durães *et al.*, *Braz. J. Phys.* **35**, 3 (2005); **28**, 505 (1998).
- [23] U. Heinz and P. F. Kolb, *J. Phys. G* **30**, S1229 (2004).
- [24] O. Kaczmarek and F. Zantow, hep-lat/0503017 and references therein; C.-Y. Wong, hep-ph/0408020 and references therein.